Scientific Research and Essays Vol. 5(22), pp. 3411-3417, 18 November, 2010
Available online at http://www.academicjournals.org/SRE
ISSN 1992-2248 ©2010 Academic Journals

Full Length Research Paper

3-D architecture and elemental composition of fluconazole treated yeast asci

Chantel W. Swart[1], Hendrik C. Swart[2], Elizabeth Coetsee[2], Carolina H. Pohl[1], Pieter W. J. van Wyk[3] and Johan L. F. Kock[1]*

[1]Department of Microbial, Biochemical and Food Biotechnology, University of the Free State, P. O. Box 339, Bloemfontein, 9300, South Africa.
[2]Department of Physics, University of the Free State, P. O. Box 339, Bloemfontein, 9300, South Africa.
[3]Centre for Microscopy, University of the Free State, P. O. Box 339, Bloemfontein, 9300, South Africa.

Accepted 19 August, 2010

In this study, sexual structures (asci) of the yeast *Nadsonia fulvescens* containing mature and fluconazole-treated malformed ascospores were studied using NanoSAM in combination with transmission electron microscopy (TEM). This is the first application of NanoSAM to biological material. TEM exposed a variety of malformed ascospores in asci treated with fluconazole. Here some ascospores produced degenerated spiky protuberances with relatively large inclusions carried inside wrinkled asci. Other ascospores contained no walls or protuberances and were enclosed within smooth spherical shaped asci. The majority of ascospores contained less dense hollow areas surrounded by cytoplasmic material. NanoSAM studies on these asci corroborate the TEM results although less structural detail was obtained. NanoSAM showed a decrease in element intensities during etching which assisted structural analysis of ascospore less dense hollow areas.

Key words: *Nadsonia*, asci, elemental composition, fluconazole, nanosam, transmission electron microscopy, 3-D architecture.

INTRODUCTION

Since the first electron image with a resolution higher than that obtainable with a light microscope was obtained in 1935 (Selby, 1953), there has been continual improvements in electron microscopy (EM). Consequently, many variations of EM have been developed. These include scanning electron microscopy (SEM), electron tomography (ET) for three-dimensional (3-D) imaging, correlative microscopy that integrates the imaging of live cells and EM, transmission electron microscopy (TEM), reflection electron microscopy (REM), scanning transmission electron microscopy (STEM), low voltage electron microscopy (LVEM) and energy-dispersive X-ray spectroscopy (EDS) in combination with scanning transmission electron microscopy (STEM) or SEM respectively (Hochella et al., 1986; Koster and Klumperman, 2003). The more recent combination of SEM with auger electron spectroscopy (AES) led to the development of scanning auger microscopy (SAM). SAM has the ability to perform semi-quantitative elemental analysis on volumes extremely smaller than those analyzed with SEM/EDS while the sample is visualized by SEM. SAM is usually used in the near-surface analysis of conductors and semi-conductors (Hochella et al., 1986). SAM has also been used in conjunction with targeted etching, where materials such as semi-conductors were etched with an Argon (Ar^+) gun. For the purpose of this study, SAM in combination with Ar^+ etching will be referred to as Nano scanning auger microscopy (NanoSAM). Yet so far, no mention has been made of the application of NanoSAM to biological material. Previous studies show that the antifungal fluconazole inhibits mitochondrial function in *Nadsonia* and may cause malformation of ascospores (Swart et al., Variation in mitochondrial activity over the life cycle of *Nadsonia fulvescens*. AJMR, In Press). However, detailed ultrastructural studies on malformed ascospores and associated asci have up till now not been performed.

*Corresponding author. E-mail: kockjl@ufs.ac.za. Tel: +27 51 401 2249. Fax: +27 51 444 3219.

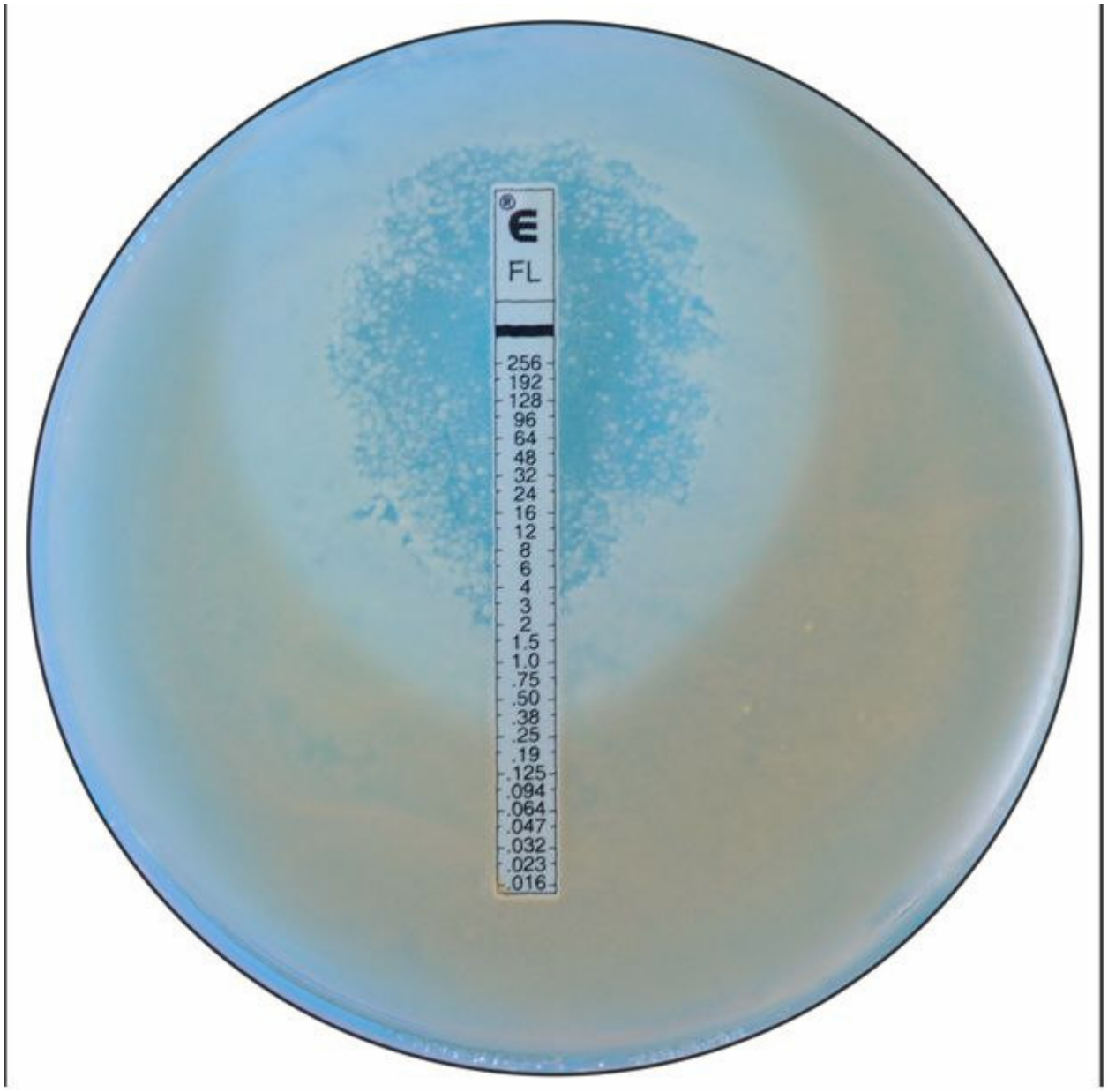

Figure 1. An antifungal bio-assay showing inhibition of cell growth (blue zone) at high concentrations of fluconazole, inhibition of mainly ascus development (white zone) at lower concentrations and eventually no inhibition of ascus development (brown zone) at still lower concentrations. (Taken from Swart et al., Variation in mitochondrial activity over the life cycle of *N. fulvescens*. AJMR, In Press).

In this study NanoSAM, in combination with TEM, was applied for the first time to investigate asci and ascospores of *N. fulvescens* treated with this antifungal.

MATERIALS AND METHODS

Yeast cells (asci) containing ascospores were prepared from the yeast *N. fulvescens* UOFS Y-0705 (obtained from the UNESCO MIRCEN yeast culture collection, University of the Free State, Bloemfontein, South Africa). To achieve this, the yeast was grown on yeast-malt (YM) agar (Wickerham, 1951) at 22°C, for 6 – 8 days, until sporulation was observed. The cells were then subjected to the following experimental procedures:

i. Fluconazole treatment: E-test strips (Davies Diagnostics, South Africa) were overlaid on agar surfaces previously covered with inocula of above yeast (Swart et al., Variation in mitochondrial activity over the life cycle of *N. fulvescens*. AJMR, In Press). Plates were incubated at 22°C for 6 – 8 days and viewed for the formation of inhibition as well as white and brown zones (Figure 1). Detailed cell analysis was performed by light microscopy (Zeiss Axioplan, Germany).

ii. Scanning electron microscopy: Cells were scraped from white (0.38 - 1.5 µg/mL fluconazole concentration region) and brown

(< 0.38 µg/mL fluconazole concentration region) zones respectively and prepared for SEM (Figure 1). In short, cells were fixed with equal amounts of buffered 3% (v/v; 0.1 mol/L) glutardialdehyde (Merck, Darmstadt, Germany) (Van and Wingfield, 1991). The suspension was then rinsed with the same buffer to remove excess aldehyde fixative and post-fixation was performed with 1% (m/v) buffered osmium tetraoxide (Merck, Darmstadt, Germany). The suspension was washed to remove excess osmium tetraoxide. Dehydration by a graded ethanol sequence 50, 70, 95 and 100% (x2) for 30 min per step followed, while centrifugation took place between each dehydration step. Drying was performed by using a critical point dryer, where after the specimens were mounted on stubs, coated with gold and viewed with SEM (Shimadzu SSX-550 Superscan, Tokyo, Japan) at 5 kV. Cells from the white and brown zones were treated in exactly the same manner.

iii. Nano Scanning Auger Microscopy (NanoSAM): Above samples were examined using a PHI 700 Nanoprobe (Japan) equipped with SAM and SEM facilities. The field emission electron gun used for the SEM and SAM analyses was set at: 2.34 A filament current; 4 kV extractor voltage and 238.1 µA extractor current. With these settings a 20 kV, 10 nA electron beam was obtained for the Auger analyses and SEM imaging. The electron beam diameter was 12 nm. The upper pressure of the electron gun unit was 8.8E-10 Torr. The pressure in the main chamber was 2.29E-10 Torr. Aperture A was used for all the measurements. The Field of View (FOV) for SEM was 8 µm and the number of frames used was 4. The Auger point analyses were obtained by using 10 cycles per survey, 1 eV/step and 20 ms per step. The Nanoprobe was also equipped with an Ar^+ ion sputtering gun set at: 2 kV beam voltage, 2 µA ion beam current and a 1 x 1 mm raster area, giving a sputter rate of about 27 nm/min. The ion emission current was set at 15 mA. An alternating sputter mode with sputter intervals of 1 min and sputter time of 2 min was used without any rotation.

iv. Transmission Electron Microscopy: Yeast material was scraped from white (0.38 - 1.5 µg/mL fluconazole concentration region) and brown (< 0.38 µg/mL fluconazole concentration region) zones respectively and chemically fixed with 0.1 M (pH 7) sodium phosphate-buffered glutardialdehyde (3%) for 3 h and then for 1.5 h in similarly buffered osmium tetroxide (Van and Wingfield, 1991). Fixed cells were embedded in epoxy resin and polymerized at 70°C for 8 h (Spurr, 1969). An LKB III Ultratome was used to cut 60 nm sections with glass knives. Sections were stained for 10 min with Uranyl acetate (Merck, Darmstadt, Germany), followed by lead citrate (Merck) (Reynolds, 1963) for 10 min. The preparation was viewed with a CM 100 [Philips (FEI) TEM CM 100; Eindhoven, the Netherlands] at 60 kV and photographed as digital images.

RESULTS

An inhibition (poor growth), white (cells with malformed fluconazole-inhibited asci) and brown (cells with mature asci) zone formed when yeast cells were subjected to fluconazole at different concentrations (Figure 1). The brown zone formed at low fluconazole concentrations and contained fully developed, mature asci containing spheroidal ascospores (one each) with a spiky wall surrounding inclusions referred to as lipid globules (Figure 2a; Miller and Phaff, 1998). The most susceptible part of the life cycle to fluconazole was the sexual reproductive phase. Here, no mature brown ascospores within hyaline asci were observed. Instead, some ascospores produced degenerated spiky protuberances with relatively large inclusions carried inside wrinkled asci (Figures 2b, c and d). Other ascospores again contained no walls with protuberances and were enclosed within smooth spherical shaped asci (Figures 2e, f, g and h). The majority of ascospores contained less dense hollow areas surrounded by cytoplasmic material (Figure 2i).

The ion gun was used successfully to make targeted sputtered etching depth profiles of up to 1026 nm that is, about halfway into the 2.0 - 2.5 µm diameter mature (Figures 3a - f) and fluconazole-inhibited asci (Figures 3j - l). In the former, etching proceeds through shrunken cell walls of the two asci (Figure 3a) leaving bare crunched spiky appendages with irregular shape (Figure 3b). When reaching an etching depth of about 1026 nm, a solid ascospore surface was observed (Figure 3c) with remnants of the crunched spiky protuberances visible on the periphery and surrounded by the shrunken cell wall. In order to obtain an improved 3-D visualization of these spiky protuberances, the experiment was repeated on other mature asci (Figure 3d). The outer layer of the ascus wall was etched by peeling off 27 nm (Figure 3e). As etching continued to about 1000 nm into the ascus, the ascospore as well as spiny protuberances was observed in 3-D (Figure 3f). SAM element colour maps indicated a high gold (Au) intensity (Au indicated in green, Figure 3g; corresponding to Figure 3d) as etching commenced. This is to be expected since the samples are covered with Au during preparation, to make it more electrons conductive. As the outer layer of the ascus wall was etched off, carbon (C) and oxygen (O) were revealed (Au indicated in green; C indicated in blue; O indicated in red; Figure 3h; corresponding to Figure 3e). Some remains of Au were also observed where etching has not yet taken place. As etching continued into the ascus, Au was no longer visible, yet a high intensity of C and some O could be observed (Figure 3i; corresponding to Figure 3f).

The cell wall surrounding the fluconazole-inhibited ascus was smooth (Figure 3j) and upon further etching a second, also smooth walled structure, with different texture became visible (Figure 3k). This 3-D structure seems to contain less dense hollow areas inside the malformed ascospore that disintegrated upon further etching (Figure 3l). This structure corresponds well to structures observed with transmission electron microscopy (Figure 2i). In order to make a quantitative assessment of the element composition as etching proceed, elemental composition depth profiles of asci during sputtering were also obtained (Figure 4). A drastic decrease in Au and Os intensities was evident when reaching an etching depth of 135 nm into asci suggesting that these elements are associated mainly with asci outer cell walls thereby also diluting C intensities substantially (sputter time = 0 min; Figures 4b and d). The F content (indicates fluconazole since it contains F or fluorine) remained at low intensities throughout etching of the malformed asci (Figure 4d), while F was absent in the control mature asci (Figure 4b). This was to be expected

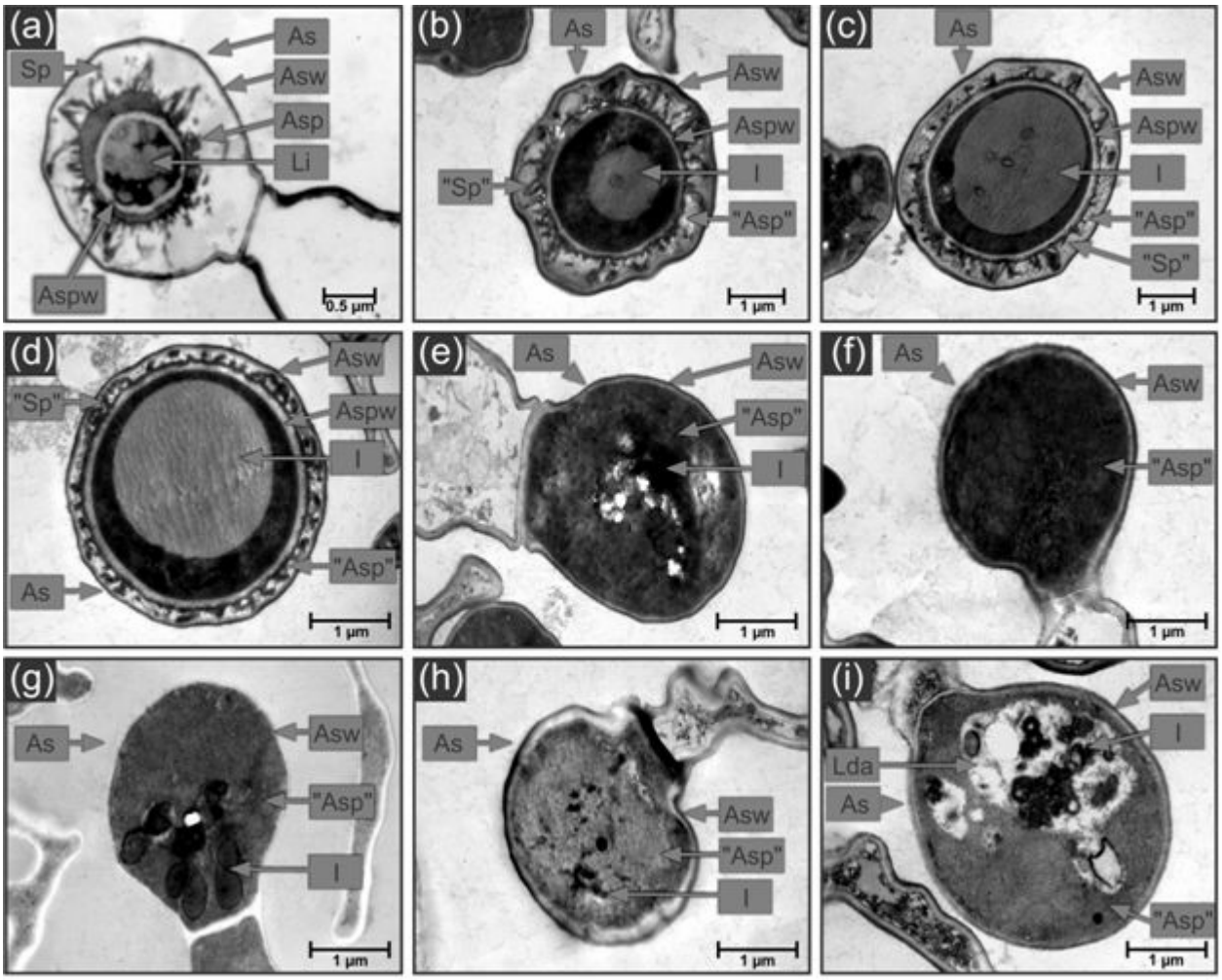

Figure 2. Transmission electron microscopy micrographs indicating the various effects of fluconazole on ascospore development of *N. fulvescens*. (a), Ascus containing a single mature ascospore with spiky protuberances. (b - d), Ascospores that produced degenerated spiky protuberances with relatively large inclusions carried inside wrinkled asci. (e - h), Ascospores containing no walls or protuberances and enclosed within smooth spherical shaped asci. (i), Ascospore containing less dense hollow areas surrounded by cytoplasmic material. As = ascus; Asp = ascospore; “Asp” = malformed ascospore; Aspw = ascospore wall; Asw = ascus wall; I = inclusions; Lda = less dense area; Li = lipid inclusions; Sp = spiky protuberances; “Sp” = degenerated spiky protuberances.

since yeasts can not produce compounds containing F. F can therefore be used as a marker to detect the presence of the antifungal fluconazole in yeast cells. In both cases, trace amounts of N could be observed (results not shown).

Different C/O intensity ratios were observed during etching through asci (Figure 4). The mature asci (target point 3; Figures 4a and b) were characterized by relatively high C/O ratios throughout etching while the malformed ascus (target point 2; Figures 4c and d) was characterized by a decrease in C/O ratio. These results were reproducible when repeated on target sites 1, 2 and 4 (Figure 4a). In addition, a significant decrease in C intensity occurred as etching proceeded in malformed ascospores (Figure 4d). The cell wall onto which target point 1 was projected was not considered since limited etching occurred (Figure 4c). These results correspond well with the scanning auger microscopy element maps of similar etched asci (Figures 3g – i). The observed pulsing (repetitive increase and decrease of elemental intensities; Figures 4b and d) is ascribed to changes in chemical structures and concentrations as etching proceed through asci inclusions.

DISCUSSION

In 2007, Kock and co-workers showed that the oxygen-dependent sexual stages of yeasts are most sensitive to mitochondrial inhibitors and are therefore selectively targeted. This suggests that mitochondrial inhibitors may also serve as antifungals by inhibiting yeast spore

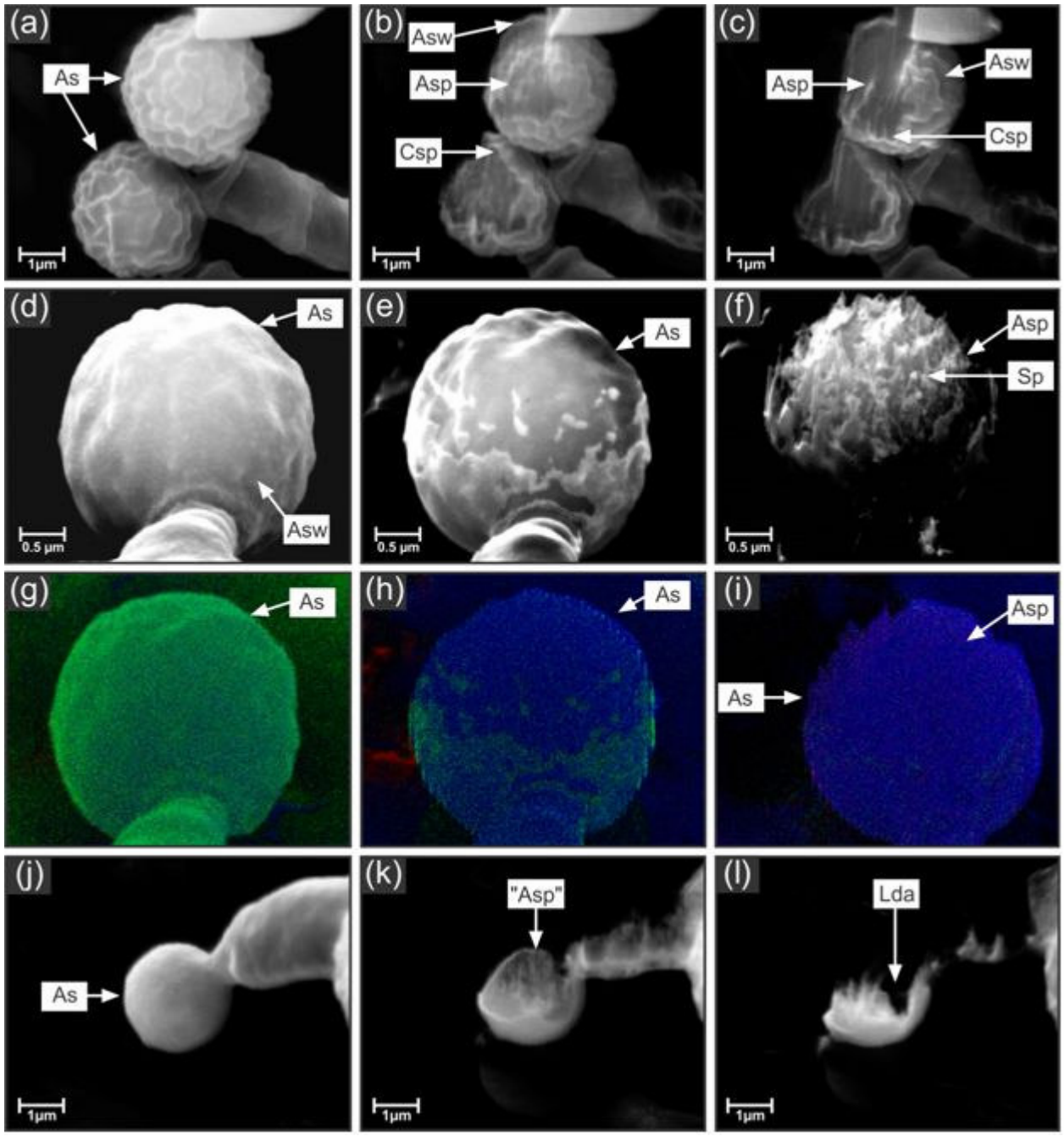

Figure 3. Scanning electron microscopy micrographs at different stages of sequential targeted etching into asci (As) of *N. fulvescens* developed in the presence of various concentrations of the antifungal fluconazole. (a - f), sequential etching through spiky ascospores (Asp) within shrunken asci (As) from the brown zone. (g - i), colour maps of the various elements present in the sample. These maps correspond to the etching micrographs (d - f). Blue – carbon (C), Green – gold (Au), Red – oxygen (O). (j - l), scanning electron microscopy micrographs at different stages of sequential targeted etching into asci (As) of *N. fulvescens* developed in the presence of higher concentrations of fluconazole indicating a less dense area (Lda) beneath the ascus wall. “Asp” = malformed ascospore; Asw = ascus wall; Csp = crunched spiky protuberances; Sp = spiky protuberance.

dispersal. To further test the general validity of this hypothesis, the antifungal fluconazole this is also regarded as a mitochondrial inhibitor (Swart et al., Variation in mitochondrial activity over the life cycle of *N. fulvescens*. AJMR, In Press), were further studied for its ability to selectively target sexual reproduction of the yeast *N. fulvescens*. This yeast is characterized by a peculiar type of sexual reproduction where each sexual

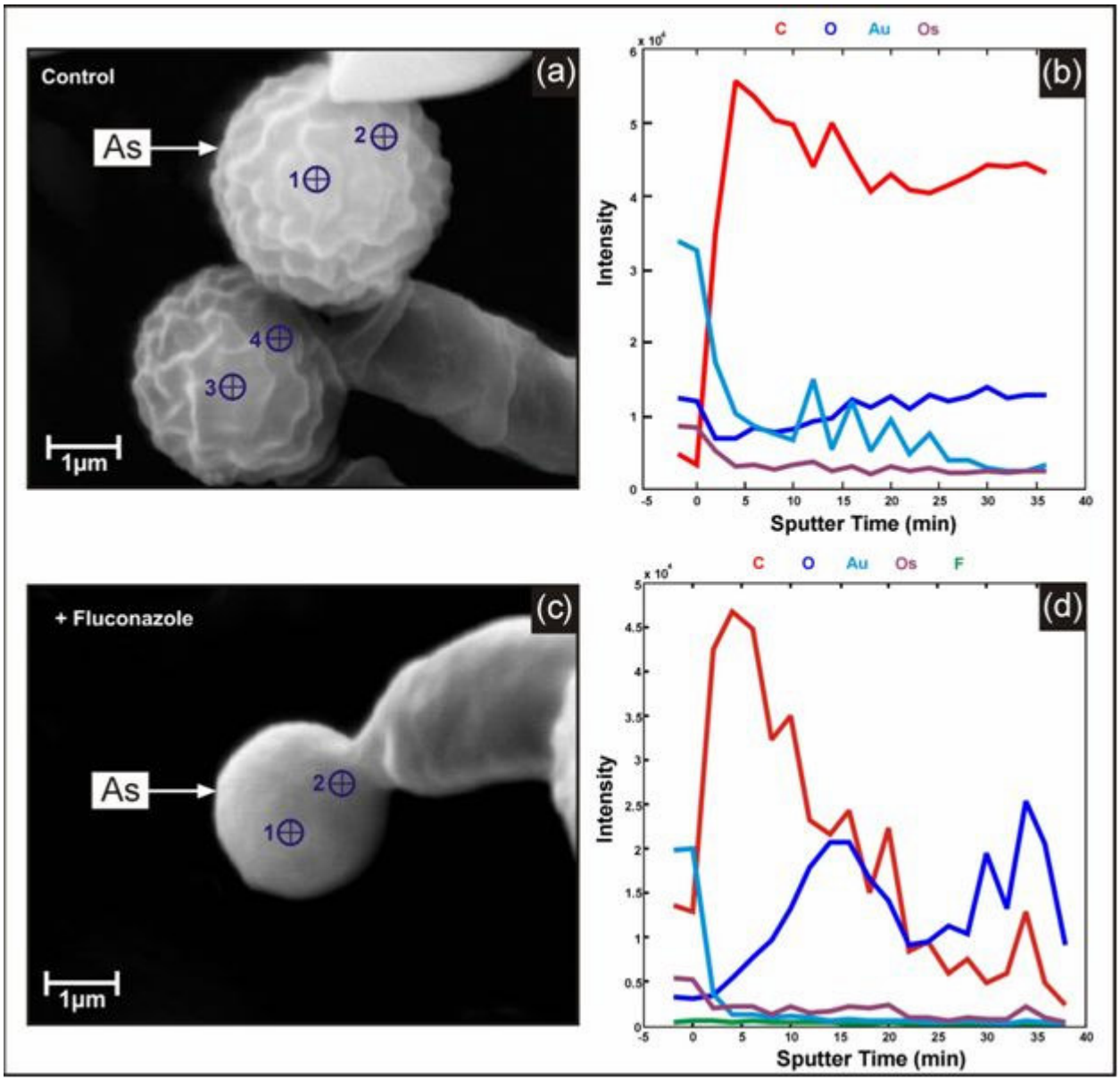

Figure 4. Elemental analysis through asci (As) during sequential etching. (a), SEM micrograph of two asci from brown zone, each attached to a parental cell (control). The targets for elemental analysis are indicated by crossed circles. (b), A graph showing elemental intensity over sputter time of control sample in (a) (Target 3). (c), SEM micrograph of a smooth walled fluconazole treated ascus attached to a parental cell from the white zone. The targets for elemental analysis are indicated as crossed circles. (d), A graph showing elemental intensity over sputter time of a fluconazole treated ascus from the white zone (Target 2).

birth-sac (ascus) produces only one sexual spore (ascospore) with spiky protuberances enclosed within the ascus (Figure 2a; Miller and Phaff, 1998). Colonies with these sexual stages are brown in colour due to melanin-stained mature asci (Miller and Phaff, 1998).

According to the results obtained (Figures 1 and 2) it is clear that the most susceptible part of the yeast life cycle was the sexual stage, in particular ascus development. This is in accordance with literature where mitochondrial inhibitors affected similar responses in other yeasts (Kock et al., 2007). Since ascospore development was impaired in various ways (Figures 2b - i), it will be interesting to determine if these are fluconazole concentration dependent. Future studies should address this possibility. We also obtained the 3-D architecture and element composition of fluconazole-inhibited ascus structure (Figure 2i) with NanoSAM and compared this to mature asci each containing a single enclosed mature ascospore (Figure 2a). Here, SEM, nano-etching with an Argon sputter gun and also elemental analysis using a

nanoprobe was for the first time successfully applied in yeast biology. Nano-etching was achieved by sputtering the sample with ionized Argon atoms, thereby peeling 27 nm segments from the sample with every bombardment (sputtering). This enabled the detection of the 3-D nanostructure of mature and fluconazole-inhibited asci. From the results (Figures 3a-l) we conclude that fluconazole inhibits ascospore formation especially the development of spiky protuberances and causes the formation of less dense areas inside malformed ascospores. The spiny protuberances shown in Figure 3f corroborates the ascospore morphology observed using transmission electron microscopy (Figure 2a), except that some shrinkage of the ascus cell wall occurred during NanoSAM preparation, probably through dehydration giving a wrinkled appearance to the ascus. Such 3-D visualization has not been reported before for any type of biological system. The ability of these malformed ascospores to germinate as well as the induction of mutations should now be assessed.

Elemental analysis was performed by focusing the nanoprobe on a specific target site on the sample, the site was then bombarded with electrons from the nanoprobe and Auger electrons released. These Auger electrons were detected via a detector and a specific energy profile was obtained. These profiles were specific for every element and therefore the unknown elements in the sample could be identified. SAM was achieved by mapping the various elements across the etched surfaces in the sample. Here the nanoprobe scanned across the sample, indicating specific elements in specific colours. A colour map of various elements was therefore obtained for each sample surface analyzed (Figures 3g - i). Although, removal of gold from the surface by Argon etching could be clearly visualized (Figure 3h), no hint of ultrastructural structures such as organelles could be observed. This may be possible if the resolution of the different colour maps could be increased in future.

In combination with elemental analyses, this method was capable of determining the elemental composition of asci including ascospores. Changes in the elemental composition as etching proceeded through asci clearly show a drastic loss in carbon intensity towards the inside of the ascospore. This corroborates the existence of a less dense area inside the ascospores (compare Figure 4d with Figure 2i). It is interesting to note that the observed hole inside the treated ascospore (Figure 3l) was not empty but contained less dense material. Although, this could not be detected by the NanoSAM SEM mode, it was clear from the elemental analysis (Figure 4d). Therefore, elemental tracking by NanoSAM may be used to study surfaces not visible by SEM. The difference between the elemental composition of the mature and fluconazole-inhibited malformed asci can only be explained when a more detailed chemical analysis of asci is performed and the relative amounts of glutardialdehyde, chitosan, beta-glucan, melanin, mannan, etc., are known.

Conclusions

The authors conclude that fluconazole at concentrations of 0.38 to 1.5 µg/mL inhibits normal ascospore development in the yeast *N. fulvescens.* In most cases, these fluconazole treated asci produced malformed ascospores with internal less dense hollow areas. We found that NanoSAM in conjunction with TEM is capable of visualizing the 3-D architecture as well as elemental intensities of malformed and normal ascospores. Changes in element intensities, as analysed by NanoSAM, may also be useful in probing less dense areas (not visible by SEM) which are concealed within structures such as malformed ascospores. This is not possible with presently used EM and other microscopy protocols. This is an advancement in 3-D ultrastructure research methodology (Sorzano et al., 2007) with obvious wide application. The application of NanoSAM to microbial ultrastructure, systematics, animal embryonic cell development, early cancer cell detection and many more should now be assessed. The influence of different cell treatment regimes for NanoSAM on elemental analysis should also be researched.

ACKNOWLEDGEMENTS

The authors wish to thank the South African National Research Foundation (NRF) Blue Skies Research Programme (BS2008092300002) as well as SAFOI for financial support.

REFERENCES

Hochella MF, Harris DW, Turner AM (1986). Scanning Auger Microscopy as a high-resolution microprobe for geologic materials. Am. Mineralogist, 71: 1247-1257.

Kock JLF, Sebolai OM, Pohl CH, Van Wyk PWJ, Lodolo EJ (2007). Oxylipin studies expose aspirin as antifungal. FEMS Yeast Res., 7: 1207-1217.

Koster AJ, Klumperman J (2003). Review: Electron microscopy in cell biology: integrating structure and function. Nat. Rev. Mol. Cell Biol., 4: SS6-SS10.

Miller MW, Phaff HJ (1998). *Nadsonia* Sydow. In Kurtzman et al. (eds) The Yeast – a Taxonomic Study, 4th ed, Elsevier Science Publication BV, Amsterdam, The Netherlands, pp. 268-270.

Reynolds ES (1963). The use of lead citrate at high pH as an electron opaque stain in electron microscopy. J. Cell. Biol., 17: 208-212.

Selby CC (1953). Microscopy II. Electron Microscopy: A Review. Cancer Res., 13(11): 753-775.

Sorzano COS, Jonic S, Cottevieille M, Larquet E, Boisset N, Marco S (2007). 3-D electron microscopy of biological nanomachines: principles and applications. Eur. Biophys. J., 36: 995-1013.

Spurr AR (1969). A low viscosity epoxy resin embedding medium for electron microscopy. J. Ultrastruct. Res., 26: 1-43.

Van Wyk PWJ, Wingfield MJ (1991). Ascospore ultrastructure and development of *Ophiostoma cucullatum*. Mycologia, 83: 698-707.

Wickerham LJ (1951). Taxonomy of yeasts. Technical Bulletin No. 1029. US Department of Agriculture. Washington, D.C., USA.